Synergistic convergence of microbiota-specific systemic IgG and secretory IgA

Karim Dorgham, Hela El Kafsi, Sébastien Andre, Eric Oksenhendler, Jehane Fadlallah, Delphine Sterlin, Claire Fieschi, Christophe Parizot, Gaëlle Autaa, Pascale Ghillani-Dalbin, et al.

Synergistic convergence of microbiota-specific systemic IgG and secretory IgA

Jehane Fadlallah[1,3†], Delphine Sterlin[1†], Claire Fieschi[3], Christophe Parizot[1], Karim Dorgham[1], Hela El Kafsi[1], Gaëlle Autaa[1], Pascale Ghillani-Dalbin[1], Catherine Juste[2], Patricia Lepage[2], Marion Malphettes[3], Lionel Galicier[3], David Boutboul[3], Karine Clément[4,5,6,7], Sébastien André[4,5,6], Florian Marquet[4,5,6], Christophe Tresallet[8], Alexis Mathian[1], Makoto Miyara[1], Eric Oksenhendler[3], Zahir Amoura[1], Hans Yssel[1], Martin Larsen[1*], Guy Gorochov[1*]

Affiliations:

[1]Sorbonne Université, INSERM, Centre d'Immunologie et des Maladies Infectieuses (CIMI-Paris), AP-HP Hôpital Pitié-Salpêtrière, F-75013 Paris, France

[2]UMR1319 Micalis, INRA, Jouy-en-Josas, France.

[3]Université Paris Diderot Paris 7, Department of Clinical Immunology, Hôpital Saint-Louis, Assistance Publique Hôpitaux de Paris (APHP), EA3518, 75010, Paris, France

[4]INSERM, UMR_S 1166, NutriOmics Team, F-75013, Paris, France;

[5]Sorbonne Universités, UPMC University Paris 06, UMR_S 1166, F-75005, Paris, France;

[6]Institute of Cardiometabolism and Nutrition, ICAN, Pitié-Salpêtrière Hospital, Assistance Publique Hôpitaux de Paris, F-75013, Paris, France;

[7]Assistance Publique Hôpitaux de Paris, Pitié-Salpêtrière Hospital, Nutrition, Endocrinology Departments, F-75013, Paris, France

[8]Assistance Publique Hôpitaux de Paris, Pitié-Salpêtrière Hospital, Department of surgery, F-75013, Paris, France

[†]These authors contributed equally to this work

*To whom correspondence should be addressed: guy.gorochov@upmc.fr or martin.larsen@upmc.fr.

Conflict of interests: The authors declare no competing interests.

Funding: The study was financed by Institut national de la santé et de la recherche médicale (Inserm) and Agence Nationale de la Recherche (MetAntibody ANR)

Abstract (<250 words)

Background: Besides intestinal barrier function, the host tolerates gut commensals through both innate and adaptive immune mechanisms. It is now clear that gut commensals induce local immunoglobulin A (IgA) responses, but it remains unclear whether anti-microbiota responses remain confined to the gut.

Objective: The aim of this study was to investigate systemic and intestinal responses against the whole microbiota under homeostatic conditions, and in the absence of IgA.

Methods: We analyzed blood and feces from healthy donors, patients with selective IgA deficiency (SIgAd) and common variable immunodeficiency (CVID). Immunoglobulin-coated bacterial repertoires were analyzed by combined bacterial fluorescence-activated cell sorting and 16S rRNA sequencing, and bacterial lysates were probed by western blot analysis with healthy donors serums.

Results: Although absent from the healthy gut, serum anti-microbiota IgG are present in healthy individuals, and increased in SIgAd patients. IgG converge with non-overlapping secretory IgA repertoires to target the same bacteria. Each individual targets a diverse, microbiota repertoire whose proportion inversely correlates with systemic inflammation. Finally, Intravenous Immunoglobulin preparations (IVIG) target much less efficiently CVID gut microbiota than healthy microbiota.

Conclusion: Secretory IgA is pivotal for induction of tolerance to gut microbiota. SIgAd-associated inflammation is inversely correlated with systemic anti-commensal IgG responses, which may thus serve as a second line of defense. We speculate that SIgAd patients could benefit from oral IgA supplementation. Our data also suggest that IVIG preparations might be supplemented with IgG from IgA deficient patients pools in order to offer a better protection against gut bacterial translocations in CVID.

Key Messages:

- Systemic IgG and secretory IgA bind a common spectrum of commensals.
- Increased proportions of IgG+ microbiota and inflammatory markers in SIgAd.
- IVIG poorly target CVID and SIgAd gut microbiota.

Capsule summary:

Serum anti-microbiota IgG are present in healthy individuals, and increased in SIgAd. IVIG only bind a small fraction of SIgAd gut microbiota. Oral IgA and IgA/IgG supplementation should be considered in SIgAd and CVID, respectively.

Key words (<10): gut microbiota, anti-commensal IgG, secretory IgA, IgA deficiency, CVID, IVIG.

Abbreviations:

Ig: Immunoglobulin

SIgAd : Selective IgA deficiency

CVID: Common Variable Immunodeficiency

IVIG: Intravenous Immunoglobulin

Acknowledgments: The authors wish to thank Emma Slack for advice, Jean-Michel Batto for discussions, Joel Doré, Fabienne Beguet-Crespel and Emma Slack for providing bacterial strains.

Funding: The study was financed by: Institut national de la santé et de la recherche médicale (Inserm), Agence Nationale de la Recherche (MetAntibody, ANR-14-CE14-0013), Fondation pour l'Aide a la Recherche sur la Sclérose En Plaques (ARSEP).

Introduction

Gut commensal bacteria contribute to several beneficial properties to the host. This complex community provides metabolic functions, prevents pathogen colonization and enhances immune development. A symbiotic relationship is maintained using host innate and adaptive immune responses such as antimicrobial compounds and mucus secretion, as well as IgA production [1,2]. However, the gastrointestinal tract remains an important reservoir for potential bloodstream infections that involve *Enterobacteriaceae*, *Enterococcus* species or other Gram-negative bacilli [3,4]. The physical gut barrier, but also innate and adaptive immune mechanisms, control host-microbiota mutualism, reducing the risk of bacterial translocation and systemic immune activation. Murine models of innate immune deficiency indeed develop high seric IgG levels against gut microbiota [2]. Significant titers of IgG targeting *E. coli* were also reported either in patients with inflammatory bowel diseases or in mice lacking secretory IgA [5,6]. Nevertheless, based on recent murine studies, the notion has emerged that induction of systemic IgG responses against gut symbiotic bacteria is not necessarily a consequence of mucosal immune dysfunction or epithelial barrier leakiness. Healthy mice actively generate systemic IgG against a wide range of commensal bacteria under homeostatic conditions, which are passively transferred to the neonates through the maternal milk [7]. Serum IgG that specifically recognize symbiotic Gram-negative bacteria confer protection against systemic infections by these same bacteria. Because such IgG target a conserved antigen in commensal and pathogens, they also enhance elimination of pathogens such as Salmonella [8].

IgG-expressing B cells are present in human gut lamina propria during steady state conditions, and represent 3-4% of the total gut B cells. About two-third of IgG+ lamina propria antibodies react with common intestinal microbes [9]. Inflammatory bowel disease is associated with a marked increase in gut IgG^+ B cells that might contribute to the observed elevated serum anti-*E. coli* IgG levels in these patients [9]. However, to which extent gut IgG^+

B cells contribute to the serum IgG repertoire, remains elusive. Focusing on anti-transglutaminase 2 antibodies, it has been shown a low degree of clonal relationship between serum and intestinal IgG [10]. Altogether, it remains unknown whether secretory and serum anti-bacteria antibodies have identical targets or whether digestive and systemic antibody repertoires are shaped by distinct microbial consortia.

In this study, we report that human serum IgG bind a broad range of commensal bacteria. We also demonstrate for the first time the convergence of intestinal IgA and serum IgG responses toward the same microbial targets, under homeostatic conditions. Private anti-microbiota IgG specificities are induced in IgA-deficient patients, but are not found in IgG pools from healthy donors, partially explaining why substitutive IgG cannot regulate antibody deficiency-associated gut dysbiosis and intestinal translocation. Finally, in both controls and IgA-deficient patients, systemic anti-microbiota IgG responses correlate with reduced inflammation suggesting that systemic IgG responses contribute to the gut microbiota confinement.

Results

1/ Convergence of intestinal IgA and serum IgG toward the same bacterial cells

To determine the level of humoral systemic response against fecal microbiota, we have elaborated a flow cytometric assay derived from a previously reported technology [11]. This protocol allows to probe concomitantly IgA and IgG microbiota coating. We found that approximately 8% of the fecal microbiota is targeted by secretory IgA (median[min-max]%; 8[0.8-26.7]%; n=30) in healthy donors, in concordance with previous reports [12]. As shown, the proportion of bacteria *in vivo* bound by secretory IgA in human feces is highly variable between healthy individuals (Figure 1B). IgG-bound bacteria are virtually absent from healthy human feces (median [min-max]%; 0.03[0-0.16]%; n=30 ; Figure S1 and 1A), in agreement with the lack of IgG transport to the intestinal lumen. In healthy donors, seric IgG bound a median rate of 1.1% of fecal bacteria (median [min-max]%; 1.1[0.2-3.2]%; Figure 1B). Surprisingly, seric IgG targeted exclusively secretory IgA bound bacteria (Figure 1A). Conversely, all IgA-coated bacteria (IgA^+ bacteria) were not targeted by seric IgG. Of note, an irrelevant human monoclonal IgG (chimeric anti-human TNF containing a human Fc IgG fraction) exhibits markedly reduced binding to IgA+ bacteria, compared to serum IgG (Figure 1A, S2), demonstrating that IgG binding to IgA-coated bacteria is mostly Fab-mediated.

To confirm that systemic IgG binding is directed against IgA-bound bacteria, we evaluated *in vitro* serum IgG binding to cultivable bacterial strains. We selected four bacterial strains that were not preferentially bound by IgA in human feces and four others that were previously defined as classical IgA targets *in vivo* [12–14]. As shown in Figure 2, IgG from healthy individuals (n = 30) bind much more significantly *Bifidobacterium longum, Bifidobacterium adolescentis, Faecalibacterium prausnitzii* and *Escherichia coli*, known to be particularly enriched in the IgA-coated fraction of healthy individuals, than three different strains of *Bacteroides sp.* and *Parabacteroides distasonis*, known to be particularly enriched in the IgA-

uncoated fraction of the fecal microbiota (Figure 2A-B). The majority of anti-commensal IgG antibodies are of the IgG2b and IgG3 isotypes in mice. Using isotype-specific secondary antibodies we detected minimal IgG1 binding, but high seric IgG2 reactivity, to *Bifidobacterium adolescentis, Bifidobacterium longum* and *Escherichia coli*, suggesting that IgG2 is involved in commensals targetting in humans (Figure S3).

Since anti-commensal IgG might possibly be triggered during mucosal immune responses, we characterized lamina propria B cells and detected the presence of IgG2+ B cells throughout the intestine (Figure S4). Of note, IgG transcripts are more abundant in LP tissue that in PBMCs, as measured by qPCR (Figure S4).

These results demonstrate that human IgG recognize a wide range of commensal under homeostatic conditions. Systemic humoral immunity (notably IgG2) converges with mucosal immunity to bind the surface of commensals.

2/ Inter-individual variability and non overlapping anti-commensal IgA and IgG molecular targets.

It was previously suggested that murine IgG would target a restricted number of bacterial proteins and favored highly conserved outer membrane proteins [8]. Reactivity of human serum IgG against bacterial lysates from a Gram-negative strains was evaluated by immunoblotting. We observed that IgG labeled several *E. coli* bands (Figure 2C), suggesting that multiple bacterial products are involved in the induction of systemic antibodies. Interestingly, this analysis reveals a great deal of inter-individual variability, as it is not always the same bacterial products that react with the tested serums. We then compared the overlap between bacterial products labeled by IgG and IgA and found distinct binding profiles (Figure 2C). Finally, in the 5 individuals tested, although some bacterial products (notably a 15 Kd

antigen) are frequently targeted in most subjects and without isotype restriction, it clearly appears that IgA and IgG never share exactly the same binding pattern at a molecular level.

Taken together, these results demonstrate although IgG converges with IgA to bind the surface of commensals, it appears that IgA and IgG do not systematically target the same bacterial antigens, even at the individual level.

3/ Private anti-microbiota IgG specificities are induced in IgA-deficient patients

The existence of seric IgG able to bind IgA-coated bacteria could equally suggest that some gut bacteria (or bacterial antigens) might cross the intestinal barrier: (i) in spite of IgA, or (ii) because of IgA. In order to explore these two putatively opposing roles for IgA, we studied the systemic anti-commensal IgG response in SIgAd. These patients had undetectable seric and digestive IgA levels while seric IgG were in the normal range[15]. Anti-microbiota IgG levels were significantly higher in SIgAd compared to controls (median [min-max]%; 3.3[0.2-20.2]% *versus* 1.1%[0.2-3.2]%; Figure 3A). Using irrelevant human IgG, we confirmed that, like in healthy donors, IgG interact with fecal bacteria in a Fab-dependent manner (Figure S2B). These data support an enhanced triggering of systemic IgG immunity against fecal microbiota when lacking secretory IgA, as shown in the murine model of polymeric immunoglobulin receptor deficiency [6].

Considering this high level of anti-microbiota IgG in SIgAd, and the similarity of SIgAd and healthy microbiota composition[15], we investigated how anti-microbiota IgG repertoires from healthy donors and IgA deficient patients were overlapping. Using polyclonal IgG from pooled serum of healthy donors, we assessed IgG-bound microbiota using either healthy or SIgAd purified microbiota. We showed that pooled polyclonal IgG and autologous healthy sera recognized a similar percentage of fecal bacteria (median [min-max]%;1[0-3.7] % *vs* 1.1[0.2-3.2]%, respectively, figure 3B-C). In contrast, pooled polyclonal IgG bound a smaller

bacterial fraction of IgA deficient-microbiota compared to autologous patient serum (median [min-max]%;0.4[0-3.6] % *vs* 3.3[0.2-20.2] %, figure 3B-C). In order to test whether similar specificities are induced in all or most IgA deficient individuals, we compared their IgG reactivity to autologous or heterologous gut microbiota. In this experiment (Figure 3D), each IgA-deficient microbiota was incubated either with autologous serum (*i.e.*: autologous condition), or with serum from an unrelated IgA deficient individual (*i.e.*: heterologous condition). As shown in Figure 3D, no significant difference was seen between autologous or heterologous conditions (median autologous IgG+ microbiota 1.2% *versus* median heterologous IgG+ microbiota 1.4%). Of note, heterologous seric IgG also predominantly interact with fecal microbiota in a Fab-dependent manner (Figure S2C).

This set of data suggests that peculiar anti-microbiota IgG specificities are induced in IgA-deficient patients, but not in healthy individuals.

4/ IgG specifically recognize a broad spectrum of bacteria

To more deeply decipher anti-commensal IgG specificities in both healthy donors and IgA deficient patients, we next performed a stringent flow-sorting to isolate IgG-bound bacteria and identified their taxonomy by 16S rRNA sequencing (Figure 4A). We observed extensive inter-individual variability at genus level irrespective of immunological status (healthy donors *vs* IgA deficient patients). Microbial diversity calculated by Shannon index varied between donors, but on average bacterial diversity of IgG^+ and IgG^- bacteria was not significantly different (Figure 4B). We postulated that IgG might preferentially interact with dominant taxa, and therefore compared relative abundance of IgG-bound and IgG-unbound genera. Both fractions exhibited equal distributions of rare and abundant genera (Figure 4C), thus IgG target commensals irrespectively of their frequency. Interestingly, we found that individual IgG^+ and IgG^- fecal bacterial profiles were remarkably different, supporting a strong IgG bias against peculiar taxa that cannot be explained by an expansion of the latter. Besides, anti-

commensals IgG were not restricted to pathobionts, but also targeted symbiotic genera such as *Faecalibacterium,* whose the most common species (*i.e.: F.prausnitzii)* has been assigned anti-inflammatory properties in both healthy donors and IgA deficient patients (Figure 4D-E) [16]. From this part we conclude that anti-commensal IgG recognize a diverse array of both pathobionts and commensal bacteria. Importantly, each individual harbored a private IgG antimicrobial signature.

5/ High anti-microbiota IgG levels correlate with reduced systemic inflammation

Microbiota-specific serum IgG responses contribute to symbiotic bacteria clearance in periphery and maintain mutualism in mice [2]. We thus hypothesized that anti-commensals IgG might influence the balance of systemic inflammatory versus regulatory responses in humans. Hence, we measured plasma levels of sCD14 (a marker of monocyte activation, [17]) and observed that seric IgG-coated bacteria inversely correlated with soluble CD14 ($r=-0.42$, $p<0.005$; Figure 5A) in both healthy donors and SIgAd patients. These results are in line with the finding that IgG replacement therapy reduced endotoxemia [18]. To further explore the potential link between anti-microbiota IgG and systemic inflammation, we explored CVID patients (characterized by both IgG and IgA defects). These patients benefit from IVIG treatment. Yet, we show that IVIG do not efficiently bind CVID microbiota. As shown in Figure 5B, IVIG bound a reduced fraction of CVID microbiota compared to control microbiota (median [min-max]%; 0.37[0.00-1.14]% *vs* 1.06[0.00-3.7]%). We then determined plasma levels of sCD14 and IL-6 (an inflammatory cytokine reflecting T-cell activation) and evaluated the expression of PD-1 (a T-cell co-inhibitory molecule induced after activation) on CD4+ T cells. IL-6 as well as sCD14 levels were consistently higher in CVID patients than in healthy donors (IL-6, median [min-max]%, 1.8(0.7-60.1) pg/ml *versus* 0.6(0.33-2.4) pg/ml; sCD14, median [min-max]%; 2063 (590-5493) pg/ml *versus* median 2696(1147-4283) pg/ml;

Figure 5C-D). Moreover, CD45RA-PD1+CD4+ T cells tended to increase in CVID patients, as compared with healthy donors (median [min-max]%; 20.3(4.26-59.6)% versus 10(2.09-41.9)%, Figure 5E).

Altogether, in both controls and IgA-deficient patients, systemic anti-microbiota IgG responses correlate with reduced inflammation.

Discussion

Anti-commensal IgG have been described in patients with inflammatory diseases [5,19,20]. Here, we characterize for the first time a broad anti-commensal IgG response under homeostatic conditions in humans. Previous work demonstrated that symbiotic Gram-negative bacteria disseminate spontaneously and drive systemic IgG responses [8]. We show here that a diverse array of commensal bacteria, including Gram-positive and Gram-negative species, can induce systemic IgG. We show that a pathobiont like *E. coli* induce less systemic IgG responses than a presumably beneficial symbiont like *B. adolescentis* (Fig. 2B). Therefore the systemic IgG response in healthy humans does not appear preferentially driven by pathobionts, but also by commensals. In mice it has been shown that commensal microbes induce serum IgA responses that protect against sepsis[21], illustrating the consequence of systemic anti-microbial IgA binding to both pathogenic strains and commensals. We postulate that systemic anti-microbiota IgG, also mainly induced by commensals, could have the same protective role.

Strikingly, systemic IgG and secretory IgA converge towards the same autologous microbiota subset. Yet, it seems unlikely that secretory IgA enhances systemic IgG responses, since IgA deficiency is associated with high proportions of IgG+ microbiota, as detected using bacterial flow cytometry on SIgAd microbiota labeled with autologous serum. In addition, induction of anti-commensal IgG has been shown to be microbiota-dependent, but IgA-independent in mice [2,6]. Systemic IgG could reflect asymptomatic gut microbiota translocation episodes in healthy individuals. Repeated bacterial translocations might occur more frequently in the absence of secretory IgA, accounting for elevated anti-microbiota IgG levels in these patients.

IgA do not activate complement via the classical pathway [22]. Interestingly, the anti-*Bifidobacterium adolescentis* IgG response is primarily restricted to the IgG2 isotype (Figure S3), which less efficiently triggers the classical route of complement than IgG1 and IgG3 [23]. Furthermore, IgG2 poorly interact with type I FcγRs, while IgG1 and IgG3 demonstrate

affinity for most FcγRs [24]. These distinct binding patterns have functional consequences. IgG1 antibodies mediate phagocytosis and induce potent pro-inflammatory pathways while IgG2 are rather involved in dendritic cell or B cell activation [25,26]. Besides its specific Fc domain interaction, IgG2 is usually, but not exclusively, associated with anti-carbohydrate responses [27]. IgA was also recently shown to bind multiple microbial glycans [28]. Thus, IgA and IgG2 could be viewed as playing similar roles, but in different compartments. Much effort has been recently expended to develop bacterial glycan or protein microarray. Glycomics could represent a new option in order to better decipher anti-microbiota antibody targets [27,29].

Importantly, we show that IgA and IgG do not systematically target the same bacterial antigens at an individual level (Figure 2C). Therefore IgG and IgA epitopes are not strictly overlapping. This result could further illustrate antibacterial IgA/IgG synergy, and explain the absence of isotype competition allowing the observed IgA/IgG co-staining of bacteria (Figure 1).

Recent studies suggested that murine secretory IgA are polyreactive and bind a broad but defined subset of microbiota [30,31]. Similarly, up to 25% of intestinal IgG^+ plasmablasts could produce polyreactive antibodies [9]. We therefore hypothesized that the cross-reactive potential of anti-commensal IgG may act as a first line of defense against potentially harmful bacteria. In line with this idea, it can be noted that homeostatic anti-commensal IgG confer protection against pathogens such as *Salmonella* [8]. Conversely, IgG directed against *Klebsiella pneumoniae*, an opportunistic pathogen, cross-react with commensal microbes[32]. Clonally related memory B cells expressing cross-specific anti-*K. pneumoniae* antibodies were found in both lamina propria and peripheral blood in humans suggesting that generation of anti-commensal antibodies might be triggered in the mucosal compartment. At the same time, anti-commensal memory B cells might recirculate in periphery[32]. Altogether, it appears possible that bacteria-specific IgG would arise from the gut, as all bacteria-specific IgG

316 isotypes we characterized in human sera are also present in the gut (Fig. S4), and also because
317 a large proportion of gut IgG+ B cells are expected to be commensal-specific[9]. However, it
318 remains presently unknown whether serum IgG responses mainly originate from the gut
319 and/or are induced the periphery following bacterial translocation.
320 We report that each individual harbors a private set of anti-commensal IgG in both healthy
321 donors and IgA deficient patients. Since our analysis was limited to 3 IgA deficient patients,
322 further study might precisely reveal how SIgAd anti-commensal IgG bind a distinct set of
323 commensals. While IVIG preparations contain an extended set of anti-commensal IgG, we
324 observe that IVIG less efficiently bind CVID microbiota. These observations are consistent
325 with reported alterations of gut microbiota in CVID patients [33]. Microbiota perturbations are
326 also associated with selective IgA deficiency. The latter perturbations are less pronounced
327 than in CVID, since the presence of IgM appears to preserve SIgAd microbiota diversity[15].
328 Nevertheless, IgA deficiency condition is also associated in severe cases with bacterial
329 translocation, colitis and dysbiosis. These complications are not accessible to substitutive Ig
330 replacement therapy [34]. Indeed, IVIG do not appear to contain high-enough concentrations as
331 well as appropriate specificities of anti-commensal IgG. As shown in Figure 3, healthy
332 control serum usually less efficiently binds IgA deficient microbiota than autologous serum.
333 Similarly, IVIG poorly targets CVID gut microbiota (Figure 5B). In addition, local mucosal
334 antibody responses might be important in regulating microbiota composition in a way that
335 cannot be substituted by IVIG. These findings expand our understanding of how IVIG fail to
336 treat gastro-intestinal symptoms in CVID and IgA deficient patients. Dysbiosis and gastro-
337 intestinal complications might not accessible to substitutive Ig replacement therapy, since, as
338 we show, healthy IgG repertoire does not contain adequate “dysbiotic-specific” antibodies.
339

It was recently shown in mice that maternally-derived anti-commensal IgG dampen aberrant mucosal immune responses and strengthen epithelial barrier [7,35]. The contribution of systemic anti-commensal IgG to the regulation of microbiota/immune homeostasis was not explored in the latter studies. Here, we show that anti-commensal IgG are negatively associated with sCD14, suggesting they might quell inflammation. In support of this, we measured higher levels of sCD14 and IL-6 in plasma of patients lacking both IgA and IgG compared to controls (Figure 5).

Altogether, these data suggest that systemic IgG and intestinal IgA cooperate in different body compartments to limit systemic pro-inflammatory pathways. While selective IgA deficient patients harbour elevated seric anti commensal IgG levels, CVID patients can not mount an appropriate IgG response. These findings suggest that : in selective IgA deficiency, microbiota confinement is obtained at the price of a strong inflammatory response, and in CVID, confinement is lost and Ig replacement therapy do not substitute for a specific autologuous IgG response. We therefore propose that IgA supplementation might have beneficial effects on gut dysbiosis and systemic inflammatory disorders associated with antibody deficiencies. IgA might be orally delivered through a carrier system allowing colon delivery. Polymers such as gellan gum or pectin, are degraded specifically by the colonic microbiota and could thus release polymer-bound IgA locally [36].

In summary, we report for the first time a systemic anti-commensal IgG response that is restricted to intestinal IgA-coated bacteria in humans. We demonstrate that in the absence of IgA, anti-commensal IgG responses are amplified and associated with reduced systemic inflammation. Finally, the present study provides new therapeutic perspectives based on IgA

supplementation in patients with CVID or SIgAd, while SIgAd -derived IgG supplementation might be considered in CVID.

Materials and Methods

Human samples

Fresh stool and blood samples were simultaneously collected from n=30 healthy donors, n=15 selective IgA deficiency and n=10 common variable immunodeficiency patients.

Healthy donors were recruited among laboratory staff and relatives. Patients followed for clinical manifestations associated with antibody deficiencies were recruited from two French clinical immunology referral centers (Department of Clinical Immunology at Saint Louis hospital and Department of Internal Medecine at Pitié-Salpêtrière hospital, Paris). Patient's inclusion criteria were (i) undetectable seric IgA levels (<0,07 mg/mL) in at least three previous samples in the past year (ii) either selective IgA deficiency (n=15 selective IgA deficient patients), or associated with IgG and/or IgM deficiency integrating a global antibody production defect (n=10 CVID patients). Clinical and biological data were collected at inclusion time.

Surgical samples from histologically normal intestine were obtained from twelve donors undergoing gastric bypass or tumorectomy at Pitié-Salpêtrière hospital, Paris.

Oral and written consent were obtained from patients and healthy donors before inclusion in the study.

PBMC and plasma

30 mL of blood were collected in ACD tubes (BD Vacutainer®) and PBMC were isolated by density gradient procedure (Ficoll 400, Eurobio, Les Ulis, France) and then stored in liquid

nitrogen after soft freezing in isopropanol. Supernatants were collected as plasma and immediately stored at -80°C.

Stool collection and whole microbiota purification

Stool were collected immediately after emission in a container allowing anaerobic bacteria preservation (Anaerocult band, Merck, Darmstadt, Germany), aliquoted in a CO2-rich 02-low atmosphere and stored at -80°C. Fecal microbiota were extracted by gradient purification in anaerobic conditions (Freter chamber) as previously described [37]. Briefly, thawed feces were diluted in 1x-PBS (Eurobio), 0,03% w/v sodium deoxycholate (NaDC), 60% w/v Nycodenz (Sigma-aldrich, St Louis, USA) and loaded on a continuous density gradient obtained by a freezing-thawing cycle of a Nycodenz solution. Fecal bacteria were obtained after ultracentrifugation (14567 x g, 45 min, +4°C) (Beckman Coulter ultracentrifuge, swinging rotor SW28) and washed three times in 1x-PBS (Eurobio), 0,03% w/v sodium NaDC. The final pellet was diluted in 1xPBS-10%Glycerol, immediately frozen in liquid nitrogen and then stored at -80°C.

Bacterial Flow Cytometry

Specific seric antibodies levels against purified microbiota or cultivable strains were assessed by a flow cytometry assay as previously described [11]. Briefly, 10^7 bacteria (purified microbiota or cultivable strains) were fixed in a solution of 4% paraformaldehyde and simultaneously stained with a cell proliferation dye (eFluor 450, eBiosciences, CA, USA). After washing with 1mL of a 1x-PBS solution, cells were resuspended to a final concentration of 4.10^8 bacteria/mL in a 1x-PBS, 2% w/v BSA, 0.02% w/v Sodium azide solution. Then 10^7 bacteria were incubated in a 96-V bottom well plate with a 10µg/mL IgG solution (from either human serum or pooled human IgG Hizentra® - CSL Behring France or human anti-

TNF Remicade® - MSD France) per condition. Immune complexes were washed twice with a 1x-PBS, 2% w/v BSA, 0.02% w/v Sodium azide (200 µL/well, 4000 x g, 10 minutes, +4°C) and then incubated with secondary conjugated antibodies, either isotype controls mix or goat anti-human IgA-FITC and goat anti-human IgG-A647 (Jackson Immunoresearch Laboratories, West Grove, USA). Acquisition of the cells events was performed on a FACS CANTO II flow cytometer (Becton Dickinson) after washing and analysis was performed with Flow-Jo software (Treestar, Ashland, USA). Medians of fluorescence were used to measure the seric IgG response levels against the cultivable strains. Intestinal IgA binding was quantified by the same assay without incubation with seric immunoglobulins. Results are expressed as median, minimum and maximum percentages throughout the manuscript.

Cytokines quantification

IL-6 and IL-10 were measured in the serum using a 3-step digital assay relying on Single Molecule Array (Simoa) technology HD-1 Analyzer (Quanterix Corporation, Lexington, USA). Working dilutions were 1/4 for all sera in working volumes of 25µL. Lower limit of quantification for IL-6 and IL-10 are respectively of 0.01, 0.021 pg/mL.

Soluble CD14 quantification

Soluble CD14 was quantified in plasma (400-fold dilution) by ELISA (Quantikine® ELISA kit, R&D, Minneapolis, USA). Experimental procedure followed the manufacturer's recommendations. Lower limit of quantification for soluble CD14 is of 6 pg/mL.

Peripheral blood mononuclear cell phenotyping

T cell phenotyping was performed using a combination of the following antibodies : CD3-H500, CCR7-PE-Cy7, CD4-APC-Cy7 (BD Biosciences), CD45RA-PercP Cy5.5 (e-

Bioscience), CD8-A405 (Invitrogen), CD279-APC (BioLegend). Acquisition of cells events was performed using a FACS CANTO II flow cytometer (Becton Dickinson) and analysis was performed using the Flow-Jo software (Treestar).

Intestinal B cells phenotyping

Lamina propria was digested by collagenase A (Roche) in RPMI (Life Technologies) for 30 minutes at 37°C. Lymphocytes were purified by centrifugation over Ficoll 400 (Eurobio) and stained with the following antibodies: anti-CD45 APC-H7, anti-CD19 BV421, anti-IgD FITC, anti-CD27 PE-Cy7 (all purchased from BD Biosciences), and anti-IgA PE (Jackson Immunoresearch), or anti-IgG1 PE, anti-IgG2 AF488, anti-IgG3 A647 (Southern Biotech). Dead cells were excluded with LIVE/DEAD^{TM} Fixable Aqua Dead Cell Stain Kit (Invitrogen). Acquisition of cells events was performed using a FACS CANTO II flow cytometer (Becton Dickinson) and analysis was performed using the Flow-Jo software (Treestar).

Analysis of IgG-coated bacteria

Purified microbiota (10^9/condition) was washed in 1x-PBS and stained with isotype control (A647-conjugated Goat IgG, Jackson Immunoresearch Laboratories) as a negative control or anti-human IgG-A647 (Jackson Immunoresearch Laboratories). Acquisition and sorting were performed on a 2 lasers- 2 ways Fluorescent-activated cell sorter (S3 cell sorter, Bio-Rad Laboratories, California, USA). 10^6 bacteria per fraction were collected and immediately stored at -80°C as dry pellets. Purity for both fractions was systematically verified after sorting with a minimum rate of 80%. Genomic DNA was extracted and the V3–V4 region of the 16S rRNA gene was amplified by semi-nested PCR. Primers V3fwd (+357): 5' TACGGRAGGCAGCAG 3' and V4rev (+857): 5' ATCTTACCAGGGTATCTAATCCT 3'

464 were used during the first round of PCR (10 cycles). Primers V3fwd and X926_Rev (+926) 5'
465 CCGTCAATTCMTTTRAGT 3' wre used in the second PCR round (40 cycles). Polymerase
466 chain reaction amplicon libraries were sequenced using a MiSeq Illumina platform (Genotoul,
467 Toulouse, France). The open source software package Quantitative Insights Into Microbial
468 Ecology (QIIME) [38] was used to analysed sequences with the following criteria: (i) minimum
469 and maximum read length of 250 bp and 500 bp respectively, (ii) no ambiguous base calls,
470 (iii) no homopolymeric runs longer than 8 bp and (iv) minimum average Phred score > 27
471 within a sliding window of 50 bp. Sequences were aligned with NAST against the
472 GreenGenes reference core alignment set (available in QIIME as
473 core_set_aligned.fasta.imputed) using the 'align_seqs.py' script in QIIME. Sequences that did
474 not cover this region at a percent identity > 75% were removed. Operational taxonomic units
475 were picked at a threshold of 97% similarity using cd-hit from 'pick_otus.py' script in
476 QUIIME. Picking workflow in QUIIME with the cd-hit clustering method currently involves
477 collapsing identical reads using the longest sequence-first list removal algorithm, picking
478 OTU and subsequently inflating the identical reads to recapture abundance information about
479 the initial sequences. Singletons were removed, as only OTU that were present at the level of
480 at least two reads in more than one sample were retained (9413 ± 5253 sequences per
481 sample). The most abundant member of each OTU was selected through the 'pick_rep_set.py'
482 script as the representative sequence. The resulting OTU representative sequences were
483 assigned to different taxonomic levels (from phylum to genus) using the GreenGenes database
484 (release August 2012), with consensus annotation from the Ribosomal Database Project naïve
485 Bayesian classifier [RDP 10 database, version 6 [39]. To confirm the annotation, OTU
486 representative sequences were then searched against the RDP database, using the online
487 program seqmatch (http://rdp.cme.msu.edu/seqmatch/seqmatch_intro.jsp) and a threshold
488 setting of 90% to assign a genus to each sequence.

Immunoblotting

10^8 CFU of wild type *Escherichia coli* were freezed (-80°C) and thawed (37°C) three times in 30µL of lysis buffer (50mM Tris-HCL, 8M urea). Lysis efficiency was verified by Gram staining. Proteins were separated using 4%-20% polyacrylamide gel electrophoresis (Mini-PROTEAN TGX Stain-Free Precast Gels; Bio-Rad) in reducing conditions (dithiothreitol DTT and sodium dodecyl sulfate SDS, Bio-Rad) and transferred to nitrocellulose. Membranes were incubated with 10µg/ml of human seric IgG or IgA of different healthy donors. Human IgG were detected with horseradish peroxidase-conjugated goat anti-human IgG used at 1:50,000 or goat anti-human IgG used at 1:20,000 followed by enhanced chemi-luminescence revealing reaction (Clarity™ Western ECL, Bio-Rad). Human IgA were detected with horseradish peroxidase-conjugated goat anti-human IgA used at 1:20 000 (Bethyl Laboratories). All incubations were in 1x-PBS with 5% non fat milk and washing steps in 1x-PBS with 0.1% Tween.

IgG gene expression analysis

Total RNA of jejunal lamina propria fraction and PBMC were extracted with the RNeasy Mini kit (QIAGEN). cDNAs were synthesized from and prepared with M-MLV reverse transcriptase (Promega). SYBR green primers were designed by manufacturer (Roche) and used for qRT-PCR using the 7300 real time PCR system (Applied Biosystem). Data were normalized to ribosomal 18S RNA.

Figure legends:

Figure 1: Systemic IgG and secretory IgA recognize a common spectrum of commensals.

A. Representative flow cytometry dot plot showing from bottom to top isotype control, endogenous secretory IgA (without serum), human IgG anti-TNF (10µg/ml ; irrelevant IgG) and autologous systemic IgG (10µg/ml) to fecal microbiota in a healthy donor.

B. Flow cytometry analysis of the fraction of fecal microbiota bound by either secretory IgA, seric IgG or both in healthy donors (n=30). Median values are indicated and subgroups are compared with a non-parametric Mann-Whitney test.

Figure 2 : Systemic IgG bind a broad spectrum of commensals

A. Flow cytometry analysis of serum IgG binding to cultivated bacterial strains. Grey histograms represent isotype controls and dark lines anti-IgG staining.

B. Flow cytometry analysis of serum IgG binding levels to 8 different bacterial strains in healthy donors (n=30). Blue strains (left) are typically poorly coated by secretory IgA from healthy individuals while pink strains (right) are representative of typical IgA targets[15]. Results are presented as Δ Median Fluorescence Intensity (MFI) *i.e.*: IgG = MFI IgG serum – MFI IgG negative control. Red bars show medians. Kruskal-wallis test was used to calculate p-value.

C. Representative immunoblotting of *Escherichia coli* lysates probed with five different healthy human serums, with a normalized IgA and IgG levels. Ponceau staining indicates total amounts of bacteria lysates loaded. IgA and IgG binding were assessed by an HRP conjugated secondary antibody.

Figure 3: IgA deficient patients harbour private anti-commensal IgG responses.

A. Flow cytometry analysis of fecal microbiota bound by autologous seric IgG in healthy donors (n=30) and IgA deficient patients (n=15). Red bars represent medians. P-value was calculated by Mann-Whitney test.

B. Representative flow cytometry analysis of autologous seric IgG binding (left) or polyclonal IgG derived from pooled serum of healthy donors binding (right) to fecal microbiota. In a healthy donor (top) and in an IgA deficient patient (bottom).

C. Flow cytometry analysis of the IgG-bound fecal microbiota with IgG from autologous serum or polyvalent IgG in healthy donors (n=30) and IgA deficient patients (n=15). P-values were calculated by Wilcoxon-paired test.

D. Flow cytometry detection of IgG on IgA deficient microbiota (n=9), following incubation with autologous serum or heterologous serum from another, randomly picked, IgA deficient individual. P-value was calculated by Wilcoxon-paired test.

Figure 4: Private IgG anti-microbial signatures.

A. Sorting strategy of IgG-bound and IgG-unbound microbiota in 10 healthy donors and 3 IgA deficient patients. Composition of sorted subsets was next analysed by 16S rRNA sequencing.

B. Genera diversity in IgG+ and IgG- sorted fractions calculated by Shannon index. Dark symbols correspond to healthy donors, red symbols to IgA deficient patients.

C. Median relative abundance of genera in IgG+ and IgG- sorted fractions. Dark symbols correspond to healthy donors, red symbols to IgA deficient patients.

D. IgG responses toward the 30 most frequent genera in 10 healthy donors. IgG response to a given bacteria is expressed as a calculated IgG index (as defined in the box), outlining genera more likely serum IgG-bound in red.. Genera and individuals are grouped using a hierarchical clustering algorithm.

E. IgG responses (defined by IgG index) toward the 30 most frequent genera in 3 IgA deficient patients.

Figure 5: Microbiota specific IgG and inflammation

A. Percentage of serum IgG-bound microbiota correlated with sCD14 levels in autologous serum of healthy donors (triangles) and SIgAd patients (dark points). Spearman coefficient (r) and p-value (p) are indicated.

B. Flow cytometry analysis of IgG-bound microbiota following IVIG exposure in healthy donors and CVID patients.

C. sCD14 levels measured by ELISA in plasmas of healthy donors and CVID patients.

D. Seric IL-6 levels measured by Simoa technology in plasmas of healthy donors and CVID patients.

E. Flow cytometry analysis of CD4+CD45RA-PD-1+ lymphocytes in peripheral blood mononuclear cells of healthy donors and CVID patients. Percentage among CD4+ T cells is presented.

For all dot plots, black lines represent medians. Mann-Whitney test was used to calculate p-values (*p<0.05, ***p<0.001)

Figure S1: *In vivo* intestinal IgG binding to gut microbiota

Flow cytometry analysis of the fraction of fecal microbiota bound by intestinal IgG in healthy donors (HD; n=30) and selective IgA deficient patients (SIgAd; n=15). Pink bars represent medians.

Figure S2: Anti-commensals IgG react mostly in a Fab-dependent manner

(A-B) Flow cytometry analysis of 30 healthy (A) and 15 IgA deficient (B) fecal microbiota

588 samples incubated with seric IgG or human IgG anti-TNF ~~TNFα~~.

589 (C) Flow cytometry analysis of 10 IgA deficient fecal microbiota samples incubated with

590 heterologous seric IgG or human IgG anti-TNF ~~TNFα~~.

591 Wilcoxon-paired test was used to calculate p-values. **p<0.01;***p<0.001; ****p<0.0001

592

593 **Figure S3: Anti-commensals IgG are mostly of IgG2 isotype**

594 A. Representative flow cytometry analysis of serum IgG1, IgG2, IgG3 and IgG4 binding
595 to *Bifidobacterium adolescentis*. Grey histograms represent serum from an IgG2
596 deficient patient that served as negative control, red histograms represent serum from
597 a healthy donor. This donor was scored IgG2+ and IgG1- against *Bifidobacterium*
598 *adolescentis*.

599 B. Flow cytometry analysis of IgG1, IgG2, IgG3 and IgG4 binding to *Bifidobacterium*
600 *adolescentis, Bifidobacterium longum* and *Escherichia coli* in 30 healthy donors.

601

602 **Figure S4: IgG2+ B cells are present in human gut lamina propria.**

603 A. Proportions of surface IgA+, IgG1+, IgG2+, or IgG3+ cells among lamina propria
604 CD19+CD27+IgD- switched B cells were detected by flow cytometry in jejunum (n =
605 4, pink symbols), ileum (n = 2, black symbols) or colon (n = 2, blue symbols) samples.

606 B. Cgamma transcripts were determined by RT-qPCR in lamina propria (LP) and
607 peripheral blood mononuclear cells (PBMC) from 4 severely obese patients. Results
608 are expressed as fold expression in LP over PBMC (mean ± SEM)

609

610

611

612 **References**

613

614 1. Honda K, Littman DR. The microbiota in adaptive immune homeostasis and disease.
615 Nature. 2016;535:75.
616 2. Slack E, Hapfelmeier S, Stecher B, Velykoredko Y, Stoel M, Lawson MAE, et al.
617 Innate and adaptive immunity cooperate flexibly to maintain host-microbiota mutualism.
618 Science. 2009;325:617–20.
619 3. Donskey CJ. The role of the intestinal tract as a reservoir and source for transmission
620 of nosocomial pathogens. Clin Infect Dis Off Publ Infect Dis Soc Am. 2004;39:219–26.
621 4. MacFie J. Current status of bacterial translocation as a cause of surgical sepsis. Br
622 Med Bull. 2004;71:1–11.
623 5. Beaugerie L, Sokol H. Clinical, serological and genetic predictors of inflammatory
624 bowel disease course. World J Gastroenterol. 2012;18:3806–13.
625 6. Johansen FE, Pekna M, Norderhaug IN, Haneberg B, Hietala MA, Krajci P, et al.
626 Absence of epithelial immunoglobulin A transport, with increased mucosal leakiness, in
627 polymeric immunoglobulin receptor/secretory component-deficient mice. J Exp Med.
628 1999;190:915–22.
629 7. Koch MA, Reiner GL, Lugo KA, Kreuk LSM, Stanbery AG, Ansaldo E, et al.
630 Maternal IgG and IgA Antibodies Dampen Mucosal T Helper Cell Responses in Early Life.
631 Cell. 2016;165:827–41.
632 8. Zeng MY, Cisalpino D, Varadarajan S, Hellman J, Warren HS, Cascalho M, et al. Gut
633 Microbiota-Induced Immunoglobulin G Controls Systemic Infection by Symbiotic Bacteria
634 and Pathogens. Immunity. 2016;44:647–58.
635 9. Benckert J, Schmolka N, Kreschel C, Zoller MJ, Sturm A, Wiedenmann B, et al. The
636 majority of intestinal IgA+ and IgG+ plasmablasts in the human gut are antigen-specific. J

637 Clin Invest. 2011;121:1946–55.
638 10. Iversen R, Snir O, Stensland M, Kroll JE, Steinsbø Ø, Korponay-Szabó IR, et al.
639 Strong Clonal Relatedness between Serum and Gut IgA despite Different Plasma Cell
640 Origins. Cell Rep. 2017;20:2357–67.
641 11. Moor K, Fadlallah J, Toska A, Sterlin D, Balmer ML, Macpherson AJ, et al. Analysis
642 of bacterial-surface-specific antibodies in body fluids using bacterial flow cytometry. Nat
643 Protoc. 2016;11:1531–53.
644 12. Palm NW, de Zoete MR, Cullen TW, Barry NA, Stefanowski J, Hao L, et al.
645 Immunoglobulin A coating identifies colitogenic bacteria in inflammatory bowel disease.
646 Cell. 2014;158:1000–10.
647 13. D'Auria G, Peris-Bondia F, Džunková M, Mira A, Collado MC, Latorre A, et al.
648 Active and secreted IgA-coated bacterial fractions from the human gut reveal an under-
649 represented microbiota core. Sci Rep. 2013;3:3515.
650 14. Kau AL, Planer JD, Liu J, Rao S, Yatsunenko T, Trehan I, et al. Functional
651 characterization of IgA-targeted bacterial taxa from undernourished Malawian children that
652 produce diet-dependent enteropathy. Sci Transl Med. 2015;7:276ra24.
653 15. Fadlallah J, El Kafsi H, Sterlin D, Juste C, Parizot C, Dorgham K, et al. Microbial
654 ecology perturbation in human IgA deficiency. Sci Transl Med. 2018;10.
655 16. Sokol H, Pigneur B, Watterlot L, Lakhdari O, Bermúdez-Humarán LG, Gratadoux J-J,
656 et al. Faecalibacterium prausnitzii is an anti-inflammatory commensal bacterium identified by
657 gut microbiota analysis of Crohn disease patients. Proc Natl Acad Sci U S A.
658 2008;105:16731–6.
659 17. Bazil V, Strominger JL. Shedding as a mechanism of down-modulation of CD14 on
660 stimulated human monocytes. J Immunol Baltim Md 1950. 1991;147:1567–74.
661 18. Perreau M, Vigano S, Bellanger F, Pellaton C, Buss G, Comte D, et al. Exhaustion of

662 bacteria-specific CD4 T cells and microbial translocation in common variable
663 immunodeficiency disorders. J Exp Med. 2014;211:2033–45.
664 19. Landers CJ, Cohavy O, Misra R, Yang H, Lin Y-C, Braun J, et al. Selected loss of
665 tolerance evidenced by Crohn's disease-associated immune responses to auto- and microbial
666 antigens. Gastroenterology. 2002;123:689–99.
667 20. Macpherson A, Khoo UY, Forgacs I, Philpott-Howard J, Bjarnason I. Mucosal
668 antibodies in inflammatory bowel disease are directed against intestinal bacteria. Gut.
669 1996;38:365–75.
670 21. Wilmore JR, Gaudette BT, Gomez Atria D, Hashemi T, Jones DD, Gardner CA, et al.
671 Commensal Microbes Induce Serum IgA Responses that Protect against Polymicrobial
672 Sepsis. Cell Host Microbe. 2018;23:302–311.e3.
673 22. Russell MW, Mansa B. Complement-fixing properties of human IgA antibodies.
674 Alternative pathway complement activation by plastic-bound, but not specific antigen-bound,
675 IgA. Scand J Immunol. 1989;30:175–83.
676 23. Bindon CI, Hale G, Brüggemann M, Waldmann H. Human monoclonal IgG isotypes
677 differ in complement activating function at the level of C4 as well as C1q. J Exp Med.
678 1988;168:127–42.
679 24. Bruhns P, Iannascoli B, England P, Mancardi DA, Fernandez N, Jorieux S, et al.
680 Specificity and affinity of human Fcgamma receptors and their polymorphic variants for
681 human IgG subclasses. Blood. 2009;113:3716–25.
682 25. Nimmerjahn F, Gordan S, Lux A. FcγR dependent mechanisms of cytotoxic,
683 agonistic, and neutralizing antibody activities. Trends Immunol. 2015;36:325–36.
684 26. White AL, Chan HTC, French RR, Willoughby J, Mockridge CI, Roghanian A, et al.
685 Conformation of the human immunoglobulin G2 hinge imparts superagonistic properties to
686 immunostimulatory anticancer antibodies. Cancer Cell. 2015;27:138–48.

687 27. Schneider C, Smith DF, Cummings RD, Boligan KF, Hamilton RG, Bochner BS, et
688 al. The human IgG anti-carbohydrate repertoire exhibits a universal architecture and contains
689 specificity for microbial attachment sites. Sci Transl Med. 2015;7:269ra1.
690 28. Bunker JJ, Erickson SA, Flynn TM, Henry C, Koval JC, Meisel M, et al. Natural
691 polyreactive IgA antibodies coat the intestinal microbiota. Science. 2017;
692 29. Christmann BS, Abrahamsson TR, Bernstein CN, Duck LW, Mannon PJ, Berg G, et
693 al. Human seroreactivity to gut microbiota antigens. J Allergy Clin Immunol. 2015;136:1378-
694 1386-5.
695 30. Bunker JJ, Flynn TM, Koval JC, Shaw DG, Meisel M, McDonald BD, et al. Innate
696 and Adaptive Humoral Responses Coat Distinct Commensal Bacteria with Immunoglobulin
697 A. Immunity. 2015;43:541–53.
698 31. Okai S, Usui F, Yokota S, Hori-i Y, Hasegawa M, Nakamura T, et al. High-affinity
699 monoclonal IgA regulates gut microbiota and prevents colitis in mice. Nat Microbiol.
700 2016;1:16103.
701 32. Rollenske T, Szijarto V, Lukasiewicz J, Guachalla LM, Stojkovic K, Hartl K, et al.
702 Cross-specificity of protective human antibodies against Klebsiella pneumoniae LPS O-
703 antigen. Nat Immunol. 2018;19:617–24.
704 33. Jørgensen SF, Trøseid M, Kummen M, Anmarkrud JA, Michelsen AE, Osnes LT, et
705 al. Altered gut microbiota profile in common variable immunodeficiency associates with
706 levels of lipopolysaccharide and markers of systemic immune activation. Mucosal Immunol.
707 2016;9:1455–65.
708 34. Favre O, Leimgruber A, Nicole A, Spertini F. Intravenous immunoglobulin
709 replacement prevents severe and lower respiratory tract infections, but not upper respiratory
710 tract and non-respiratory infections in common variable immune deficiency. Allergy.
711 2005;60:385–90.

712 35. Gomez de Agüero M, Ganal-Vonarburg SC, Fuhrer T, Rupp S, Uchimura Y, Li H, et
713 al. The maternal microbiota drives early postnatal innate immune development. Science.
714 2016;351:1296–302.
715 36. Sandolo C, Péchiné S, Le Monnier A, Hoys S, Janoir C, Coviello T, et al.
716 Encapsulation of Cwp84 into pectin beads for oral vaccination against Clostridium difficile.
717 Eur J Pharm Biopharm Off J Arbeitsgemeinschaft Pharm Verfahrenstechnik EV.
718 2011;79:566–73.
719 37. Juste C, Kreil DP, Beauvallet C, Guillot A, Vaca S, Carapito C, et al. Bacterial protein
720 signals are associated with Crohn's disease. Gut. 2014;63:1566–77.
721 38. Caporaso JG, Kuczynski J, Stombaugh J, Bittinger K, Bushman FD, Costello EK, et
722 al. QIIME allows analysis of high-throughput community sequencing data. Nat Methods.
723 2010;7:335–6.
724 39. Cole JR, Wang Q, Cardenas E, Fish J, Chai B, Farris RJ, et al. The Ribosomal
725 Database Project: improved alignments and new tools for rRNA analysis. Nucleic Acids Res.
726 2009;37:D141-145.
727

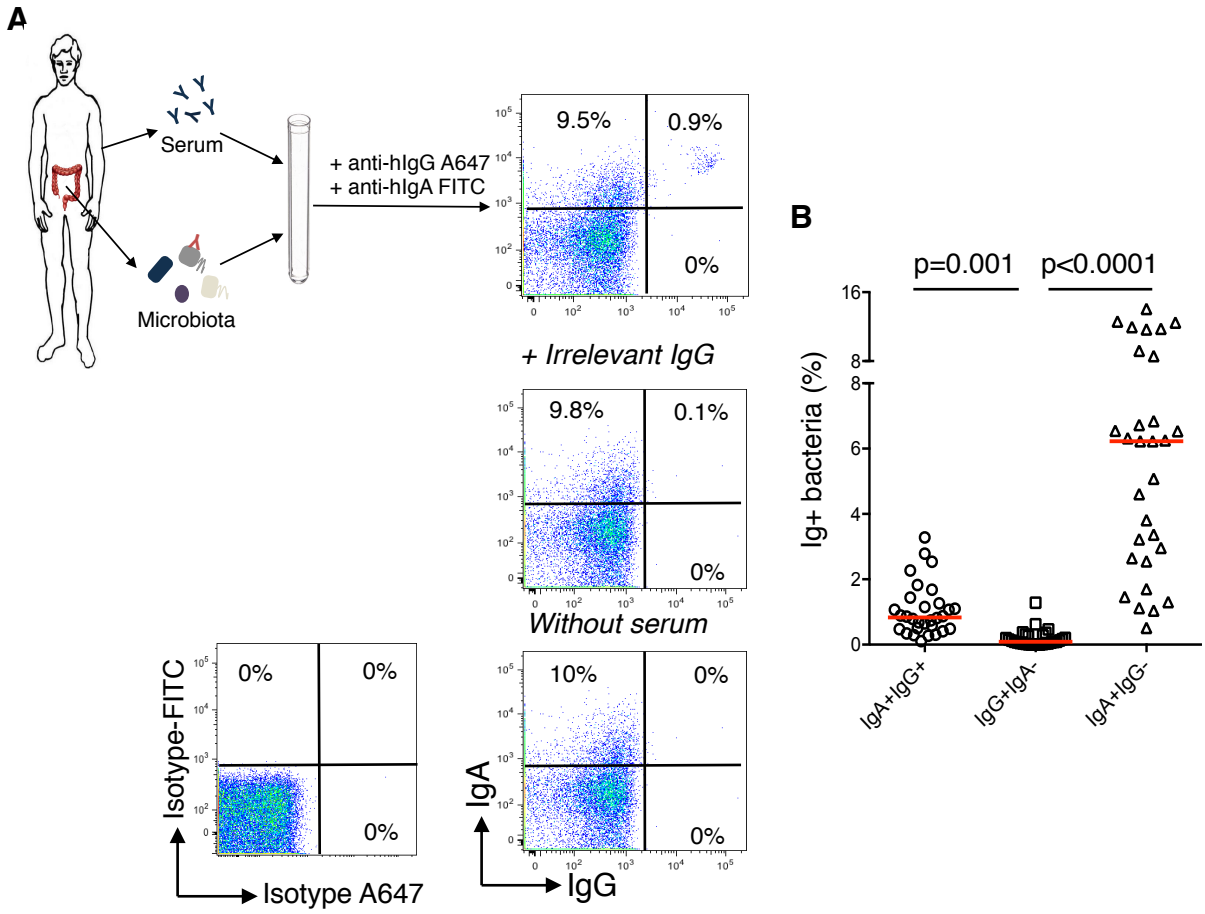
A
Serum
Microbiota
+ anti-hIgG A647
+ anti-hIgA FITC
9.5%
0.9%
0%
+ Irrelevant IgG
9.8%
0.1%
0%
Without serum
0%
0%
0%
Isotype-FITC
Isotype A647
10%
0%
0%
IgA
IgG
B
p=0.001
p<0.0001
Ig+ bacteria (%)
16
8
8
6
4
2
0
IgA+IgG+
IgG+IgA-
IgA+IgG-

Figure 1

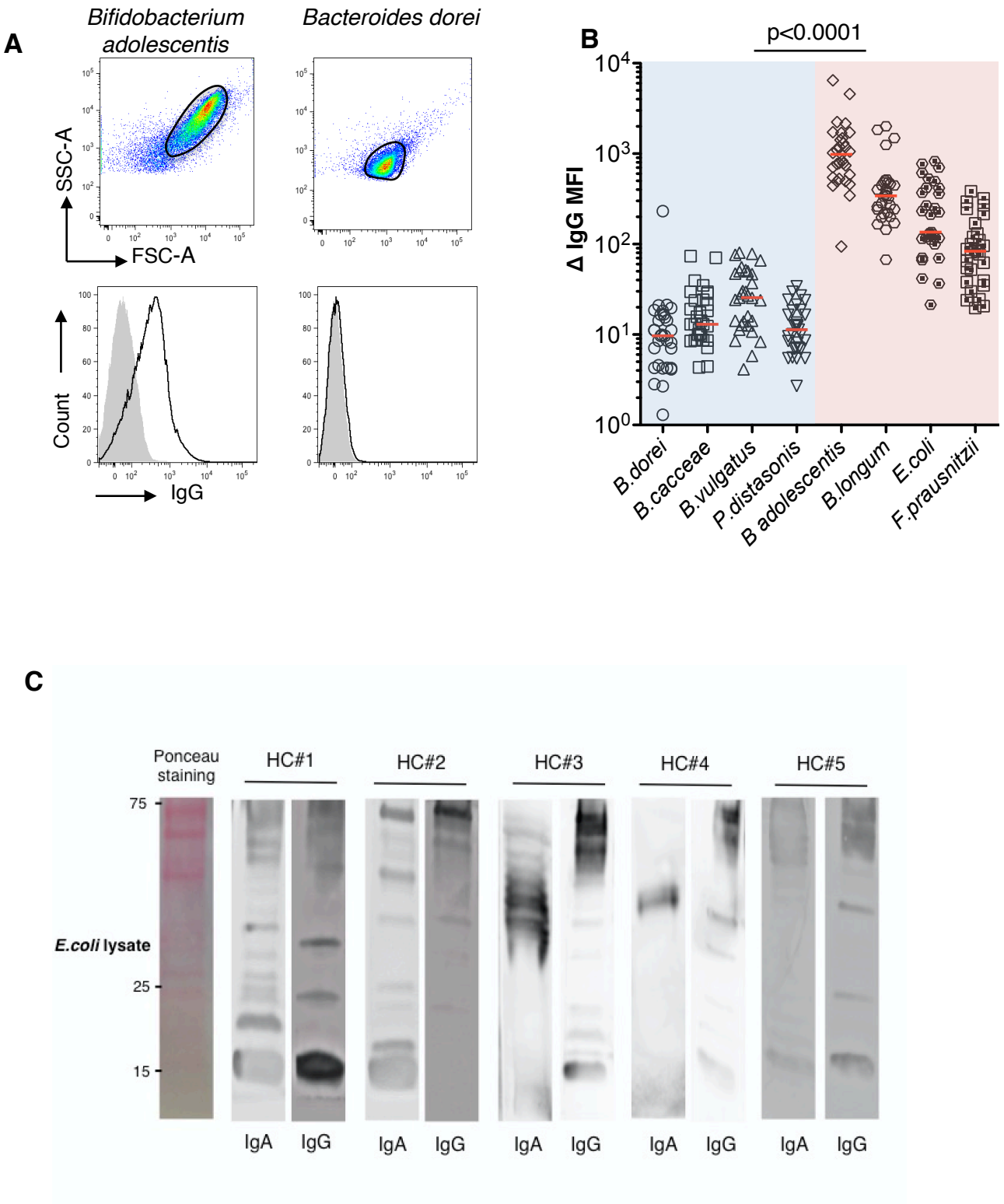
A
Bifidobacterium adolescentis
Bacteroides dorei
SSC-A
FSC-A
Count
IgG
B
p<0.0001
Δ IgG MFI
B.dorei
B.cacceae
B.vulgatus
P.distasonis
B.adolescentis
B.longum
E.coli
F.prausnitzii
C
Ponceau staining
HC#1
HC#2
HC#3
HC#4
HC#5
75
25
15
E.coli lysate
IgA
IgG

Figure 2

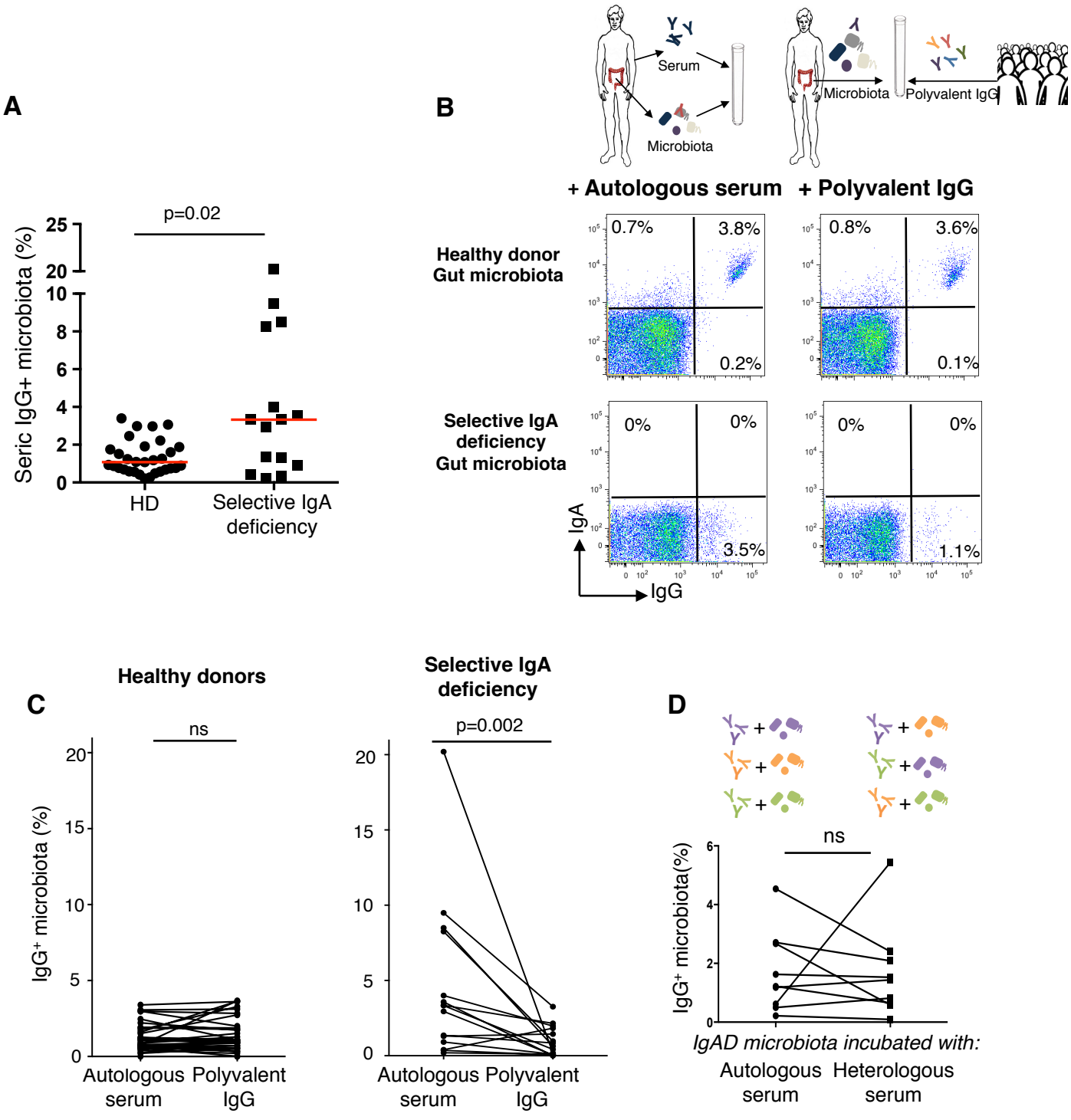
A
p=0.02
Seric IgG+ microbiota (%)
25
20
10
8
6
4
2
0
HD
Selective IgA deficiency
B
Serum
Microbiota
Microbiota
Polyvalent IgG
+ Autologous serum
+ Polyvalent IgG
Healthy donor Gut microbiota
0.7%
3.8%
0.2%
0.8%
3.6%
0.1%
Selective IgA deficiency Gut microbiota
0%
0%
3.5%
0%
0%
1.1%
IgA
IgG
C
Healthy donors
ns
IgG+ microbiota (%)
20
15
10
5
0
Autologous serum
Polyvalent IgG
Selective IgA deficiency
p=0.002
20
15
10
5
0
Autologous serum
Polyvalent IgG
D
ns
IgG+ microbiota(%)
6
4
2
0
IgAD microbiota incubated with:
Autologous serum
Heterologous serum

Figure 3

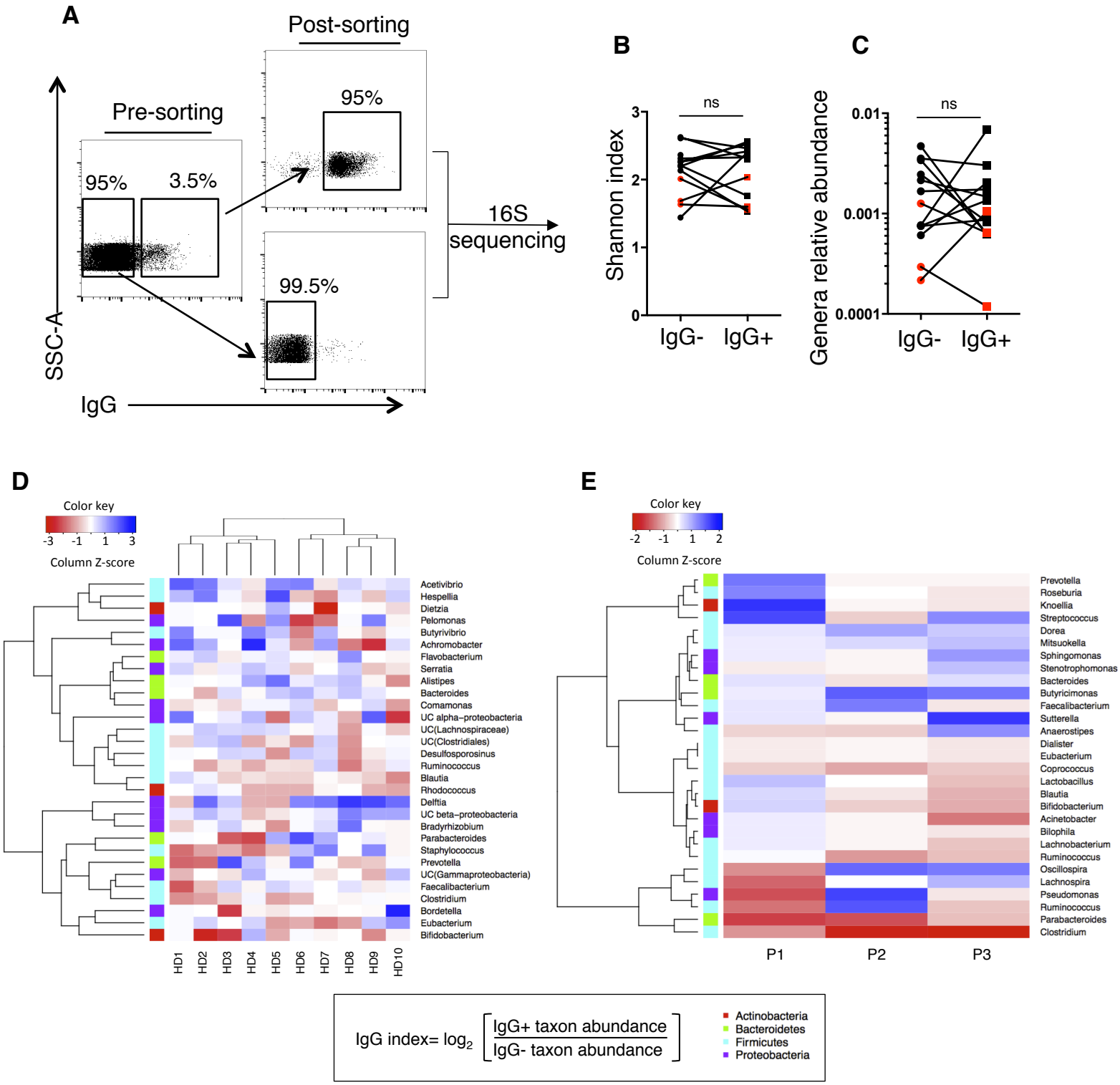
A
Post-sorting
Pre-sorting
95%
95%
3.5%
99.5%
16S
sequencing
SSC-A
IgG
B
ns
Shannon index
3
2
1
0
IgG-
IgG+
C
ns
Genera relative abundance
0.01
0.001
0.0001
IgG-
IgG+
D
Color key
-3 -1 1 3
Column Z-score
Acetivibrio
Hespellia
Dietzia
Pelomonas
Butyrivibrio
Achromobacter
Flavobacterium
Serratia
Alistipes
Bacteroides
Comamonas
UC alpha−proteobacteria
UC(Lachnospiraceae)
UC(Clostridiales)
Desulfosporosinus
Ruminococcus
Blautia
Rhodococcus
Delftia
UC beta−proteobacteria
Bradyrhizobium
Parabacteroides
Staphylococcus
Prevotella
UC(Gammaproteobacteria)
Faecalibacterium
Clostridium
Bordetella
Eubacterium
Bifidobacterium
HD1
HD2
HD3
HD4
HD5
HD6
HD7
HD8
HD9
HD10
E
Color key
-2 -1 1 2
Column Z-score
Prevotella
Roseburia
Knoellia
Streptococcus
Dorea
Mitsuokella
Sphingomonas
Stenotrophomonas
Bacteroides
Butyricimonas
Faecalibacterium
Sutterella
Anaerostipes
Dialister
Eubacterium
Coprococcus
Lactobacillus
Blautia
Bifidobacterium
Acinetobacter
Bilophila
Lachnobacterium
Ruminococcus
Oscillospira
Lachnospira
Pseudomonas
Ruminococcus
Parabacteroides
Clostridium
P1
P2
P3
IgG index= log2 [IgG+ taxon abundance / IgG- taxon abundance]
Actinobacteria
Bacteroidetes
Firmicutes
Proteobacteria

Figure 4

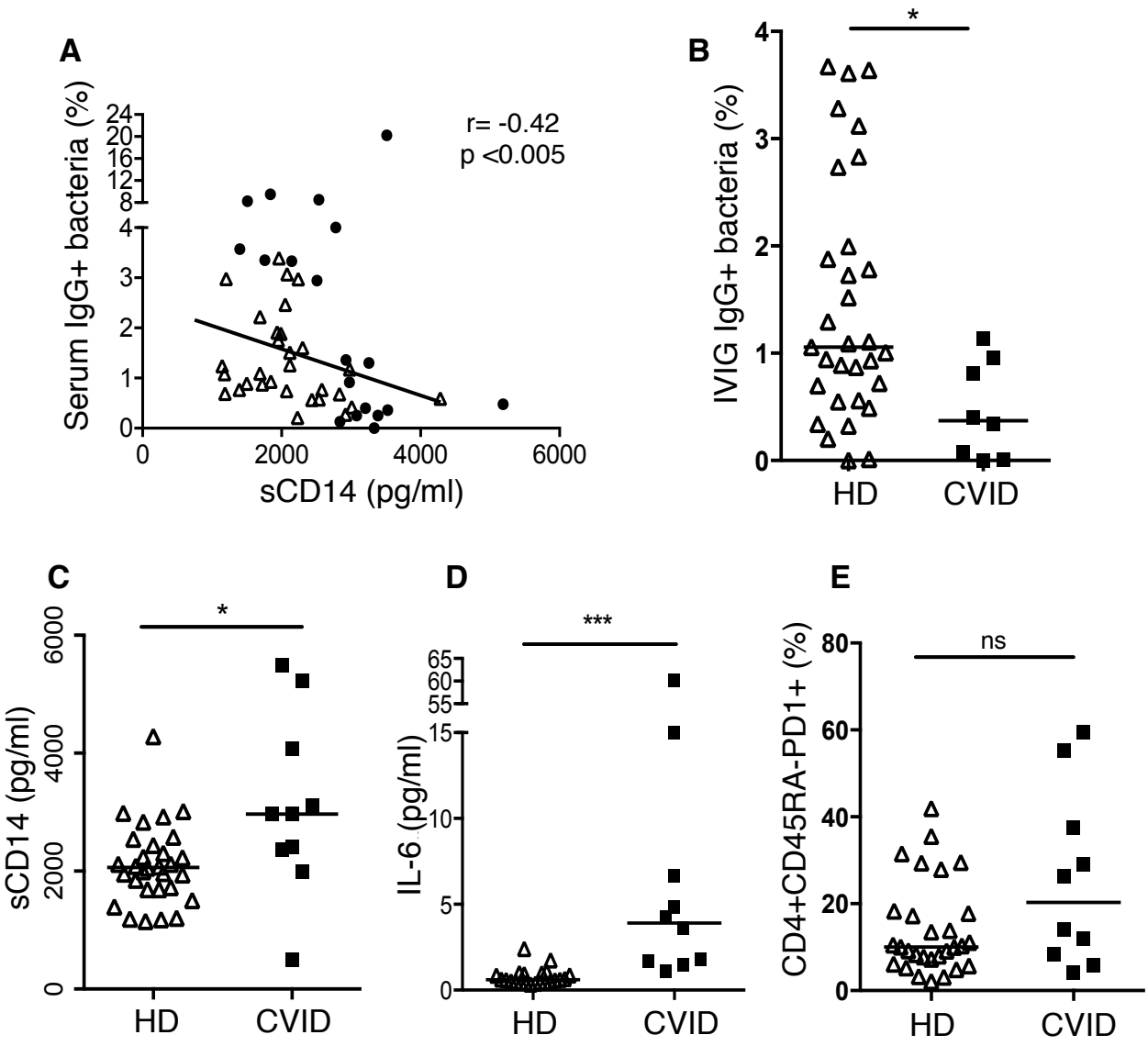
A
Serum IgG+ bacteria (%)
sCD14 (pg/ml)
r= -0.42
p <0.005
B
IVIG IgG+ bacteria (%)
HD
CVID
*
C
sCD14 (pg/ml)
*
D
IL-6 (pg/ml)
***
E
CD4+CD45RA-PD1+ (%)
ns

Figure 5

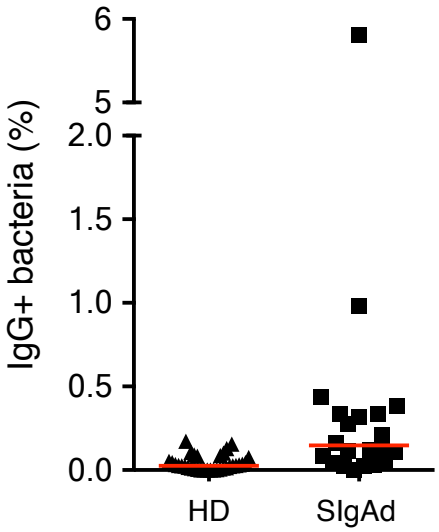

Figure S1

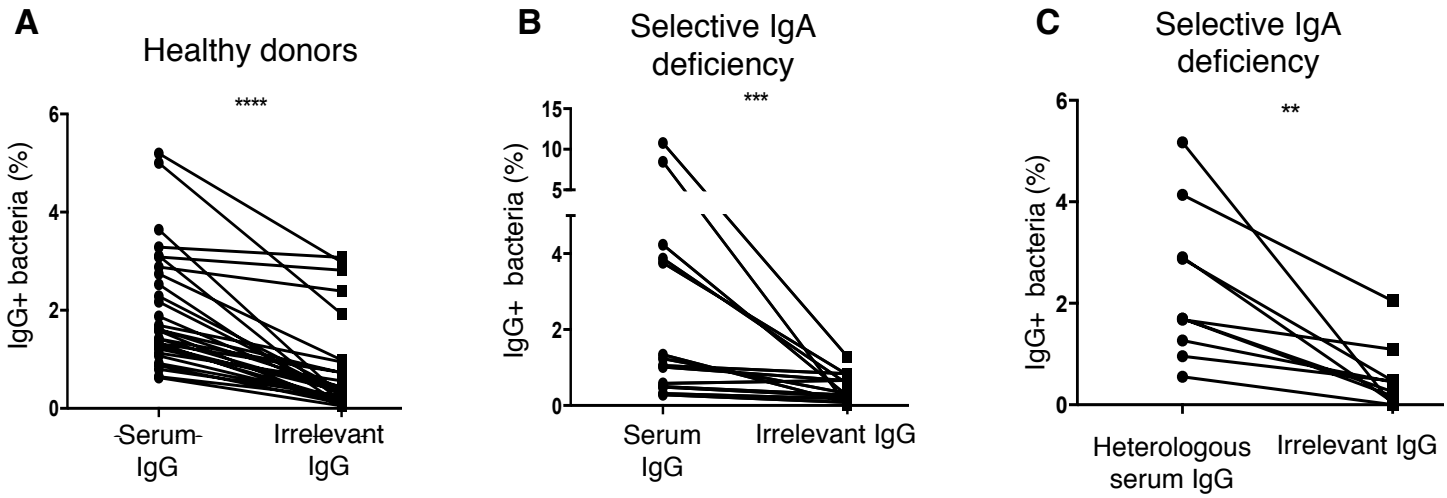

Figure S2

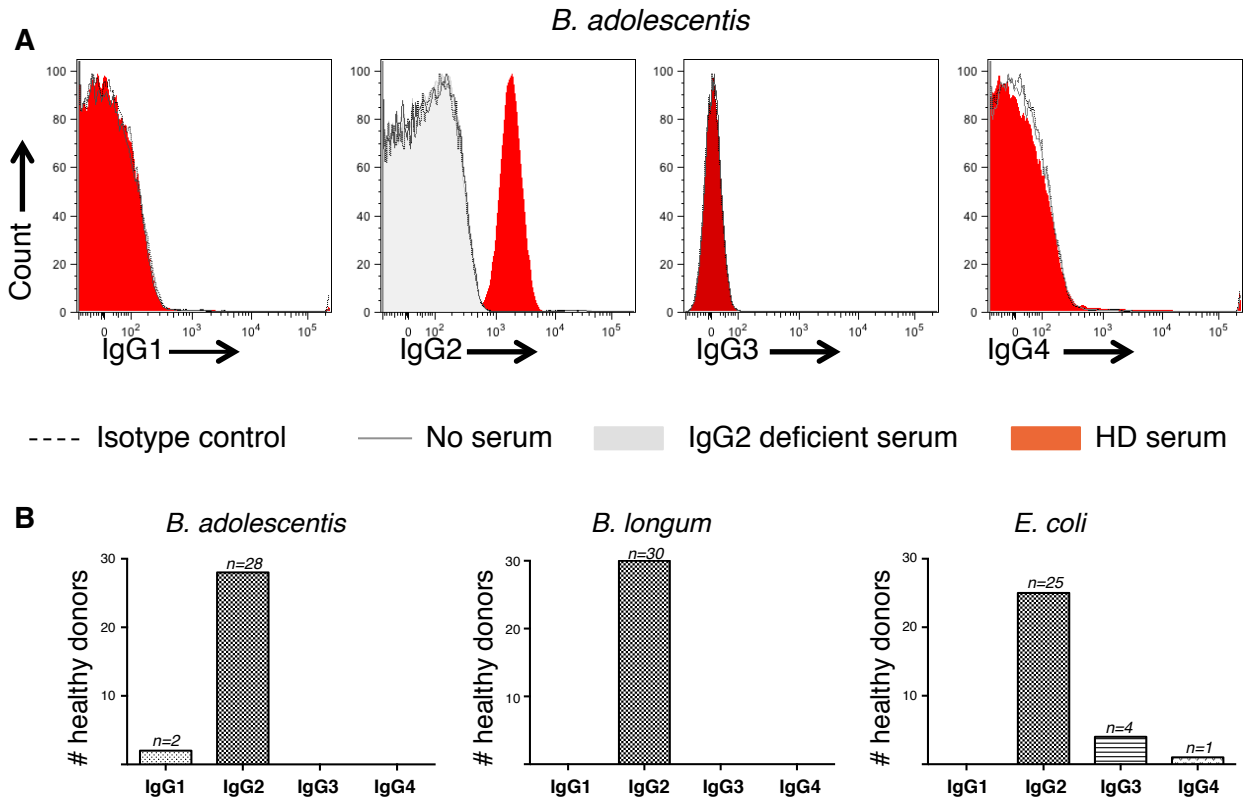
A
B. adolescentis
Count
IgG1
IgG2
IgG3
IgG4
Isotype control
No serum
IgG2 deficient serum
HD serum
B
B. adolescentis
B. longum
E. coli
# healthy donors
n=2
n=28
n=30
n=25
n=4
n=1
IgG1
IgG2
IgG3
IgG4

Figure S3

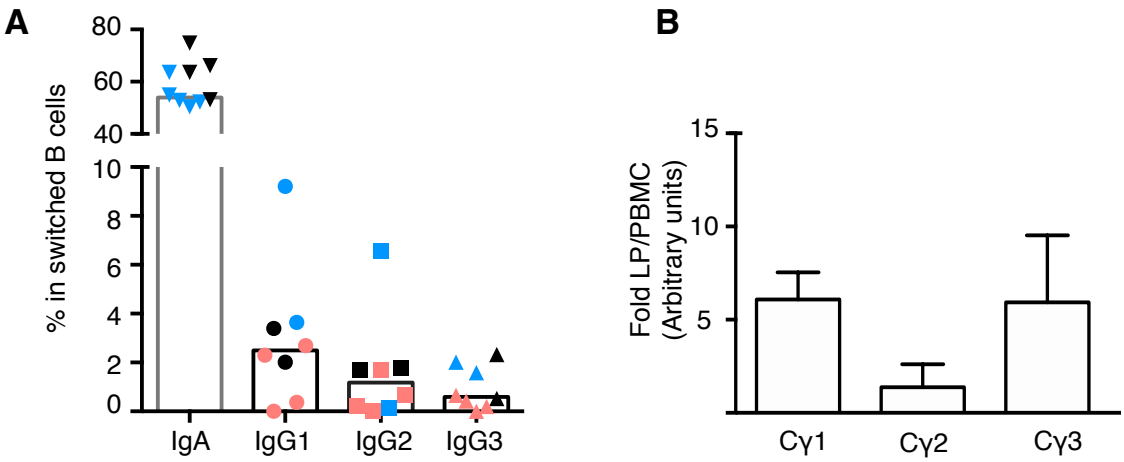
A
% in switched B cells
80
60
40
10
8
6
4
2
0
IgA
IgG1
IgG2
IgG3
B
Fold LP/PBMC
(Arbitrary units)
15
10
5
Cγ1
Cγ2
Cγ3

Figure S4